

## Suppression of Third-Order Intermodulation in a Klystron by Third-Order Injection

S. Bhattacharjee,<sup>1,\*</sup> C. Marchewka,<sup>1</sup> J. Welter,<sup>1</sup> R. Kowalczyk,<sup>2</sup> C. B. Wilsen,<sup>2,†</sup> Y. Y. Lau,<sup>2</sup> J. H. Booske,<sup>1</sup> A. Singh,<sup>1</sup>  
J. E. Scharer,<sup>1</sup> R. M. Gilgenbach,<sup>2</sup> M. J. Neumann,<sup>1</sup> and M. W. Keyser<sup>2</sup>

<sup>1</sup>*Department of Electrical and Computer Engineering, University of Wisconsin, Madison, Wisconsin 53706*

<sup>2</sup>*Department of Nuclear Engineering and Radiological Sciences, University of Michigan, Ann Arbor, Michigan 48105*  
(Received 22 October 2002; published 5 March 2003)

The first observations and measurements are reported on suppression of the third-order intermodulation (IM3) product arising from nonlinear mixing of two drive frequencies in a klystron, by externally injecting a wave at the IM3 product frequency. Optimum amplitude and phase of the injected wave for maximum suppression are examined. Results indicate that suppression of the IM3 product by as much as 30 dB can be achieved. Experimental results compare favorably with predictions of a 1D simulation code that takes into account all kinematical and dynamical effects including charge overtaking and space charge forces.

DOI: 10.1103/PhysRevLett.90.098303

PACS numbers: 84.40.Fe

Klystrons have been conventionally operated at single frequencies because of their limited bandwidth [1–4]. With the advancements in deep space and interplanetary exploration, there has been a growing interest in the possibility of multifrequency operation in a klystron. For example, the U.S. National Aeronautics and Space Administration's Jet Propulsion Laboratory has considered plans for simultaneous communication with three space probes in Martian orbit using a klystron amplifier [5]. To date, traveling wave tubes (TWTs) are more common choices for multifrequency operation due to their wider bandwidths. However, klystrons are preferred for the above applications where high powers are a major requirement. With two or more closely spaced frequencies within the available bandwidth of a typical klystron, it is a major challenge for wave amplification with minimal distortion, owing to the deleterious effects of several intermodulation products (IMPs) arising from nonlinear mixing of the drive waves. For example, with simultaneous excitation at frequencies  $f_1$  and  $f_2$ , third-order intermodulation products (IM3s) arise at  $2f_1 - f_2$  and  $2f_2 - f_1$ , whereas fifth-order intermodulation products (IM5s) with nearby frequencies arise from  $3f_1 - 2f_2$  and  $3f_2 - 2f_1$ . These intermodulation products pose a significant problem, because of their proximity to the fundamental waves being amplified [6]. As a result, they can experience a large amount of gain, eventually reaching unacceptable levels, distorting the information being transmitted, and limiting the useful data rate of the amplifier. The subject of intermodulation suppression has therefore received heightened attention in the recent past [6–15].

Injection techniques are one of the most important tools for improving amplifier linearity. For example, harmonic frequency injection has been successfully applied for both harmonic [7,8] and intermodulation distortion suppression [9] in a TWT. However, harmonic injection is not practical in a klystron because most often

the harmonic frequencies cannot be coupled to the input cavity of the klystron. In this Letter, we describe a method for the first time to suppress the IM3 by the injection of an external wave at the exact frequency of the IM3. When the injected wave is of proper phase and amplitude, a significant suppression in the distortion product IM3 is observed. The experimental results and their prediction by a simulation code [6,16] are presented.

The experiment employs a 1 kW CW Varian 4K3SL, 4-cavity klystron amplifier (KLA). The KLA operating voltage and current are approximately 6 kV and 0.6 A, respectively. It is designed to amplify signals between 1.7 and 2.4 GHz, depending upon the mechanical tuning of the cavities. The KLA was synchronously tuned to a center frequency of 1849 MHz with a 3 dB bandwidth of approximately 2.1 MHz. The tuned 4-cavity KLA provides a gain of about 45 dB at the center frequency, with saturation emerging above 79 mW input power (19 dBm). Figures 1 and 2 show the gain versus frequency and the drive curve of the klystron, respectively.

Intermodulation suppression is studied by injecting a wave at the IM3 frequency with an amplitude and phase so as to cancel the IM3 inherently produced in the tube. A design (Fig. 3) incorporating the use of a frequency doubler and a mixer was found to be most suitable for generating the required IM3 signal. Two synthesizers at  $f_1$  (1848 MHz) and  $f_2$  (1848.5 MHz) were referenced to a common 10 MHz internal generator. A portion of the signal from  $f_2$  was frequency doubled ( $2f_2$ ) so that it was phase locked to  $f_2$ . The mixer produced the  $2f_2 - f_1$  (1849 MHz IM3) wave by mixing  $2f_2$  with  $f_1$ . Thus the mixer output was phase locked to both  $f_2$  and  $f_1$  and therefore to the IM3 produced inherently in the klystron by the two fundamental drive frequencies.

The IM3 signal from the mixer was then sent through a phase shifter, allowing adjustment of the phase between the injected and the fundamental waves, and a variable attenuator for variation of the injected wave amplitude.

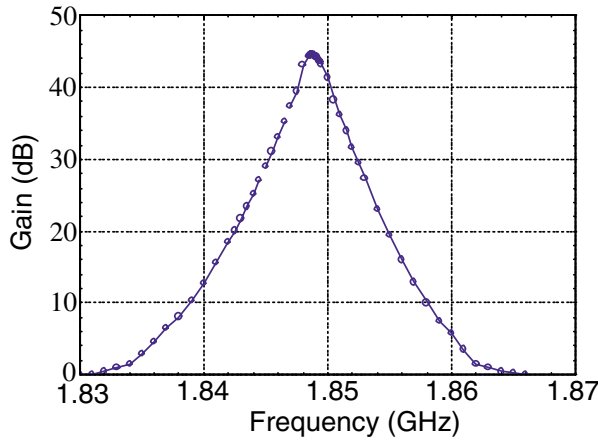


FIG. 1 (color online). Klystron small signal gain versus frequency.

Finally, if required, the injected wave was amplified before being combined with the 1848 and 1848.5 MHz fundamental drive waves using a combiner. Additional amplifiers were used in the paths of the  $f_2$  and  $f_1$  signals, respectively. The combined waves were injected into the klystron as shown in Fig. 3.

For the results presented here, the fundamental drive frequencies were independently set to approximately 158 mW (22 dB m) at the klystron input and the output spectrum was captured on an Agilent E4407B digital spectrum analyzer and a computer. The klystron output with only the drive frequencies is shown in Fig. 4. It is seen that the inherently generated IM3 product at 1849 MHz has a power level of 0.22 mW (-6.5 dBm). Next, an external 1849 MHz signal was injected at the KLA input and its phase with respect to the fundamentals was varied using the phase shifter. Figure 5 shows the sensitivity of the net 1849 MHz IM3 suppression with variation in phase of the injected IM3 signal with respect to the fundamentals. The injected IM3 amplitude level

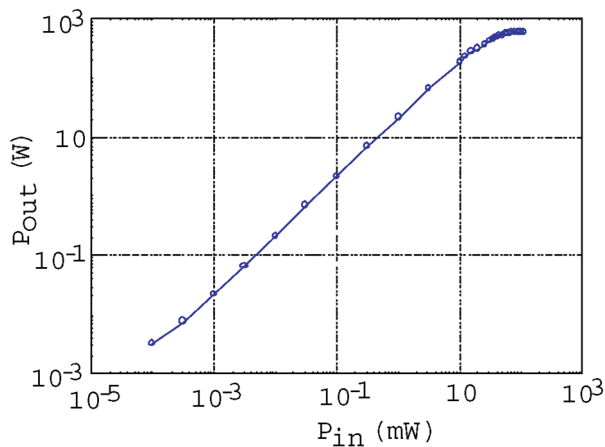


FIG. 2 (color online). Klystron drive curve (input power versus output power).

was kept fixed at a value of 0.22 mW (-6.5 dBm). The expanded view of the region around the suppression is shown in Fig. 5(b). It is noted that maximum suppression is obtained at an injected IM3 phase angle of about  $35^\circ$  with respect to the fundamentals and the power level of the IM3 at the output is reduced to  $7.1 \times 10^{-4}$  mW (-31.5 dBm). The relative suppression of the generated IM3 by the injected IM3 for these power and phase settings is therefore 25 dB. In subsequent studies, the phase angle was kept constant at  $35^\circ$  with respect to the fundamentals and the sensitivity of the IM3 output to changes in power level of the injected IM3 was studied. The result of the amplitude variation is shown in Fig. 6. The suppression was found to be quite sensitive to the injected IM3 input power and the optimum injected power for bringing about maximum suppression ( $\sim 28.9$  dB) is 0.275 mW (-5.6 dBm).

For an accurate determination of the power levels, it is critical to examine the percentage of wave reflection from the klystron input cavity to have an indication of the coupled input power. Measurements reveal that with the beam present, power reflection from the input cavity is less than 1% for frequencies within the gain bandwidth of the KLA.

The intermodulation theory of [6,16] is used to model the multifrequency excitation of the klystron. In brief, the algorithm is as follows. An rf signal consisting of an arbitrary number of drive tones, each of independent amplitude and phase, is applied to the input cavity of the klystron. An electron in the gap of the input cavity (at  $z = 0$ ) is subject to the velocity modulation

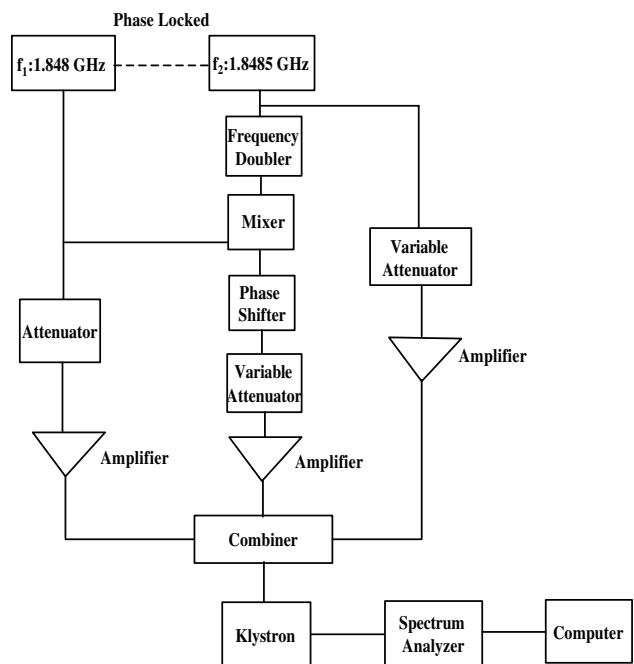


FIG. 3. Schematic of the experimental circuit.

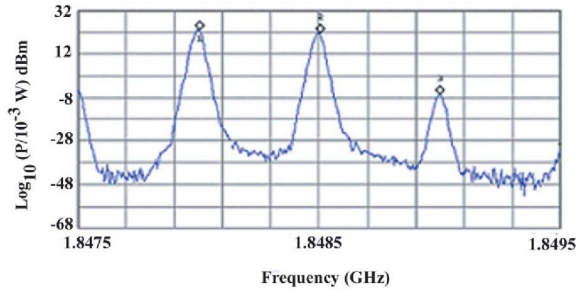


FIG. 4 (color online). Output spectra of the klystron with the two fundamental drive waves and the self generated IM3.

$$\epsilon(t_0) = \epsilon_1 \sin(\omega_1 t_0 + \theta_1) + \epsilon_2 \sin(\omega_2 t_0 + \theta_2) + \dots \quad (1)$$

Here  $\epsilon_j$ ,  $\omega_j$ , and  $\theta_j$  are, respectively, the ac gap voltage (normalized to the beam voltage), the frequency, and the phase of the  $j$ th frequency component, with  $j = 1, 2, 3, \dots$ . We assume that each input frequency is an integer multiple of some base frequency  $\omega_0$ , i.e.,  $\omega_j = N_j \omega_0$ . Then all nonlinear and intermodulation products will be integer multiples of  $\omega_0$ . In the absence

of perturbation, an electron entering the input gap at  $z = 0$  at  $t = t_0$  will arrive at distance  $z = L_1$  downstream at a later time  $t_1 = t_0 + L_1/v_0$ , where  $v_0$  is the electron drift velocity. The presence of perturbations, e.g., the multifrequency signal, the intermodulation products, the beam's ac space charge effects, and the induced gap voltage at the intervening cavities, all of which have been included in [6,16] modifies the arrival time  $t_1$  by  $\tau_1$ , and we may write the arrival time as

$$t_1 = t_1(t_0) = t_0 + \frac{L_1}{v_0} - \tau_1(t_0). \quad (2)$$

$\tau_1$  can be calculated iteratively to any desired degree of accuracy [6,16].

The total (dc + ac) current  $I_1(t_1)$  at  $z = L_1$  at time  $t_1$  subject to the orbit Eq. (2) is

$$I_1(t_1) = \sum_{n=-\infty}^{\infty} I_1(n) e^{in\omega_0 t_1}, \quad (3)$$

$$I_1(n) = I_0 e^{in\omega_0 L_1/v_0} \frac{\omega_0}{2\pi} \int_0^{2\pi/\omega_0} e^{in\omega_0 t_0 - in\omega_0 \tau_1(t_0)} dt_0. \quad (4)$$

Equation (4) describes the current modulation exactly, including intermodulation products and harmonics to all orders. It is also valid even if charge overtaking occurs [16,17].

The algorithm given above computes the modulated beam current at the output cavity in response to the velocity modulation at the input cavity. In contrast, in the physical measurement it is the input and output powers that are observed. Comparison of the computed and measured spectra requires the following calibration procedure [16].

The klystron is excited by a two-tone signal and the ratio of the fundamental frequency to the third-order intermodulation product frequency (C/IM3) is measured. The drive amplitudes should be equal and weak enough to ensure small-signal operation. The code is then used to calculate the transfer (input cavity velocity modulation versus output current modulation) curves at the fundamental C and IM3 frequencies. From the experimental

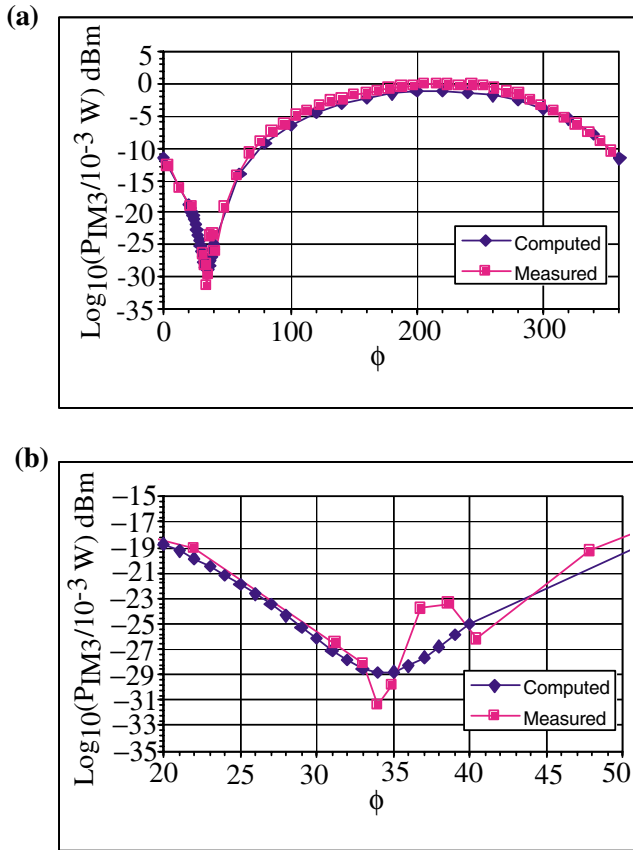


FIG. 5 (color online). (a) Sensitivity of the IM3 suppression to variation in injected IM3 phase with respect to the fundamentals; (b) Expanded view of the region around maximum suppression.

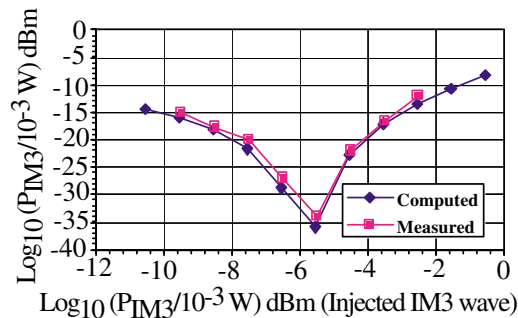


FIG. 6 (color online). Sensitivity of the IM3 suppression to variation in injected IM3 amplitude.

TABLE I. Dimensionless parameters used in the simulation.  $\omega_p$  is the reduced plasma frequency of the electron beam,  $L$  is the separation between neighboring gaps.  $N_1$  and  $N_2$  represent fundamental drive waves ( $f_1$  and  $f_2$ ), and  $N_3$  represents the injected wave at the upper IM3 frequency  $2f_2 - f_1$ .

$\epsilon_1 = \epsilon_2$	$1.1491 \times 10^{-4}$
$\theta_1 = \theta_2$	0
$N_1 = \omega_1/\omega_0$	7392
$N_2 = \omega_2/\omega_0$	7394
$N_3 = \omega_3/\omega_0$	7396
$\omega_p/\omega_1$	0.1
$\omega_p L/v_0$	0.9834

measurement of C/IM3, the calibration operating point can be located on these curves. In this way, the relation between the measured input power  $P_{in}$  and the input cavity velocity modulation,  $\epsilon$ , is determined. The conversion from the measured output power  $P_{out}$  to the computed modulated current is revealed at the same time.

For comparison with the experiment, the calibration procedure adjusts the input velocity modulation to match the experimental input power  $P_{in}$  of interest. Simulating the experiment, three excitation frequencies ( $f_1$ ,  $f_2$ , and  $2f_2 - f_1$ ) are applied. For fixed amplitude and phases at  $f_1$  and  $f_2$  the amplitude and phase of the  $2f_2 - f_1$  input excitation is varied. The effect of the variation on the output spectrum (i.e., intermodulation suppression) is studied and compared to the experimental measurements. The values of the dimensionless parameters utilized in the code are shown in Table I. The results of the simulation are shown in Figs. 5 and 6 along with those of the experiment. It is noted that excellent agreement is obtained between the two.

In conclusion, for two-tone excitation of a klystron amplifier operating near 2 GHz with a separation of 0.5 MHz, a significant reduction in the amplitude of the third-order intermodulation product results from injecting a wave at the third-order intermodulation frequency itself with an optimum amplitude and phase. Reduction of the output third-order intermodulation product power by 28.9 dB was observed for fundamental drive waves of 22 dBm/tonne. While this experiment focused on the reduction of the upper third-order intermodulation product, it is expected that adding the other tone with the appropriate amplitude and phase at the lower third-order intermodulation frequency may reduce both.

We gratefully acknowledge the support in part by AFOSR Grant No. 49620-00-1-0088 and by DUSD (S&T) under the Innovative Microwave Vacuum Electronics Multidisciplinary University Research Initiative (MURI) program, managed by the United States Air Force Office of Scientific Research under Grant No. F49620-99-1-0297 and the Northrop Grumman Industrial Affiliates Program.

\*Electronic address: sudeepb@ece.wisc.edu

†Present address: L-3 Communications Electron Devices, San Carlos, CA 94070.

- [1] R. A. Cormier and A. Mizuhara, *IEEE Trans. Microwave Theory Tech.*, **40**, 1056 (1992).
- [2] M.V. Fazio, W.B. Haynes, B.E. Carlsten, and R.M. Stringfield, *IEEE Trans. Plasma Sci.* **22**, 740 (1994).
- [3] T.G. Lee, *IEEE Trans. Electron Devices* **40**, 1329 (1993).
- [4] M. Friedman, J. Krall, Y.Y. Lau, and V. Serlin, *Rev. Sci. Instrum.* **61**, 171 (1990).
- [5] T. Cornish, "Single-Aperture Multiple-Carrier Uplink Using a 20 Kilowatt X-Band Transmitter," TMO Progress Report No. 42-144, Jet Propulsion Laboratory, Pasadena, CA, 2001.
- [6] Y.Y. Lau, D.P. Chernin, C. Wilsen, and R.M. Gilgenbach, *IEEE Trans. Plasma Sci.* **28**, 959 (2000).
- [7] W.E. Garrigus and M.I. Glick, *Microwave J.* **18**, 35 (1975).
- [8] J.J. Hamilton and D. Zavadil, *Microwave J.* **15**, 24 (1972).
- [9] M. Wirth, A. Singh, J. Scharer, and J. Booske, *IEEE Trans. Electron Devices* **49**, 1082 (2002).
- [10] D.M. Goebel, R.R. Liou, W.L. Menninger, Z. Xiaoling, and E.A. Adler, *IEEE Trans. Electron Devices* **48**, 74 (2001).
- [11] R.G. Carter, W. Bosch, V. Srivastava, and G. Gatti, *IEEE Trans. Electron Devices* **48**, 178 (2001).
- [12] C.S. Aitchinson, M. Mbabele, M.R. Moazzam, D. Budimir, and F. Ali, *IEEE Trans. Microwave Theory Tech.* **49**, 1148 (2001).
- [13] S.K. Datta, P.K. Jain, and B.N. Basu, *IEEE Trans. Electron Devices* **48**, 62 (2001).
- [14] J.G. Wohlbiel, J.H. Booske, and I. Dobson, *IEEE Trans. Plasma Sci.* **30**, 1063 (2002).
- [15] D.K. Abe, M.T. Ngo, B. Levush, T.M. Antonsen, Jr., D.P. Chernin, *IEEE Trans. Plasma Sci.* **28**, 576 (2000).
- [16] C.B. Wilsen, Ph.D. thesis, University of Michigan, 2001.
- [17] C.B. Wilsen, Y.Y. Lau, D.P. Chernin, and R.M. Gilgenbach, *IEEE Trans. Plasma Sci.* **30**, 1176 (2002).